The current issue and full text archive of this journal is available at
www.emeraldinsight.com/0332-1649.htm

Steady-state modeling of a phase-shift PWM parallel resonant converter

İres İskender
Electrical and Electronics Engineering Department, Gazi University, Ankara, Turkey, and
Yıldürüm Üçtuğ and H. Bülent Ertan
Electrical and Electronics Engineering Department, Middle East Technical University, Ankara, Turkey

Received March 2004
Revised June 2005
Accepted July 2005

Abstract

Purpose – To derive an analytical model for a dc-ac-dc parallel resonant converter operating in lagging power factor mode based on the steady-state operation conditions and considering the effects of a high-frequency transformer.

Design/methodology/approach – A range of published works relevant to dc-ac-dc converters and their control methods based on pulse-width-modulation technique are evaluated and their limitations in output measurement of higher output voltage converters are indicated. The circuit diagram of the converter is described and the general mathematical model of the system is obtained by deriving and combining the mathematical models of the different converter blocks existing in the system. The derived mathematical model is used to study the steady-state and transient performance of the converter. The deriving procedure of the analytical model for a parallel resonant converter is extensively given and the analytical model obtained is verified by simulation results achieved using MATLAB/SIMULINK and the program written by the authors.

Findings – The paper suggests an analytical model for dc-ac-dc parallel resonant converters. The model can be used in the output voltage estimation of a converter in terms of its phase-shift angle and the dc-link voltage.

Research limitations/implications – The resources in the library of the authors' university and also the English resources relative to dc-ac-dc converters reachable through the internet were researched.

Practical implications – The analytical model suggested can be used in estimating the output voltage of the converters used in high-voltage applications or where there are difficulties in employing sensors in measurement of the output voltage due to high price or implementation problems.

Originality/value – The originality of the paper is to present an analytical model for dc-ac-dc parallel resonant converters. Using this model makes it possible to estimate the output voltage of the converter using the dc-link voltage and the phase-shift angle. The proposed model provides researchers to regulate the output voltage of the converters using feed-forward control technique.

Keywords Analytical model, Power converter, High voltage, PWM

Paper type Research paper

1. Introduction

In recent years, a variety of high-frequency pulse-width-modulation (PWM) resonant tank inverter-fed dc-ac-dc converter configurations have been studied and evaluated for many specified power supply applications. The main component of these converters is

COMPEL: The International Journal for Computation and Mathematics in Electrical and Electronic Engineering
Vol. 25 No. 4, 2006
pp. 883-899

0332-1649
DOI 10.1108/03321640610684051

an inverter operating at high frequency. High frequency operation enables the whole system to adapt itself more easily to new conditions and parameter changes. In addition, high-frequency operation of the converters decreases the size and weight of converters and increases their efficiency (Sun *et al.*, 1996). An important drawback of high-frequency operation is its high switching losses that can be removed by operating the system around the resonance frequency and at lagging power factor mode.

The operation of converters at lagging power factor mode removes the disadvantages of the parallel resonant converters operating below resonance frequency, such as use of lossy RC snubbers and di/dt limiting inductances, need for fast recovery diodes across the switches (Bhat and Swamny, 1990).

Resonant converters may be classified as resonant and non-resonant couplings according to the methods of coupling between the resonant and output circuits of the converter. The converter presented in this paper is a parallel resonant converter with capacitive output filter called the non-resonant coupled (Sooksatra and Lee, 1989; Steigerwald, 1985). In the resonant converter operation, the response of the converter is determined from a sequence of different topological circuits called circuit modes. The resonant operation of a dc-ac-dc converter or the operation of a dc-ac-dc converter at unity power factor depends on both the operating frequency and the load value (Takano *et al.*, 1995; Steigerwald, 1985). The converter presented in this paper, is not operating exactly at the resonance mode (unity power factor) but is operating near resonance at lagging power mode due to the above mentioned advantages.

In high dc-voltage applications like X-ray generators, a high-turns-ratio transformer is used to increase the output voltage to the required voltage level and this implies a very large reflected secondary capacitance. Using the leakage inductance and the secondary layer capacitance of a transformer as the resonant elements of a parallel resonant converter is desirable for higher output voltage converters (Steigerwald, 1988). An important property of parallel resonant converters is that the output voltage gain is higher than one and this causes a reduction in turns-ratio of the transformer.

Feedback and feed-forward control techniques are two main control approaches used in the output voltage regulation of the converters. Though voltage regulation using feedback control technique, which requires measurement of the output voltage during operation, may be more accurate than the feed-forward technique, in some applications due to high price or implementation problems there would be difficulties in employing sensors in measurement of the output parameters. This problem can be removed using feed-forward control approach by employing a model relating the output voltage to the input parameters of the system. In this approach, the voltage regulation is achieved based on the measurement of the dc-link voltage and the adjustment of the inverter conduction angle. The deriving procedure of an analytical model for a parallel resonant converter has been extensively given in Section 4.

The phase-shift pulse-width-modulation (PSPWM) technique (see Section 3) is employed in the output voltage regulation of dc-ac-dc converters due to their wide load adjustment range. In this method, the output voltage changes from zero to its maximum value by varying the phase-shift angle of the inverter from 180 to 0° (Takano *et al.*, 1995).

The objectives of this papers are:

- to analyze and derive the dynamic mathematical models of the ac-dc and dc-ac-dc stages of the converter for different operation modes depending on the conduction states of the semiconductor switches;

- deriving a relationship between the input and output voltages of the dc-ac-dc converter based on the steady-state analysis of the converter;
- to verify the derived model using simulation results; and
- to verify the model experimentally.

2. Description of the converter circuit

The circuit described in this study is a dc-ac-dc parallel resonant converter operating at fixed frequency and controls the load voltage by PWM of the semiconductors. Figure 1 shows the block diagram of a dc-ac-dc converter connected to the ac mains through an uncontrolled rectifier. In this figure, L_1 represents the ac line inductance. The dc-ac-dc converter consists of a full bridge inverter converting the dc-link voltage into an ac voltage with square waveform. The primary winding of the high-frequency transformer is connected to the inverter and its secondary winding is connected to the load through an uncontrolled rectifier.

The inverter used in both mathematical simulation and experimental works is a single-phase full-bridge operating around the resonant frequency of the system (lagging mode) so that lossless switching of the transistors is possible during turn-on (Steigerwald, 1984).

Owing to the requirement of high voltage output, the turns-ratio of the transformer must be high, which increases the non-idealities of the transformer. To obtain an allowable insulation voltage, a sufficient geometrical distance is required between primary and the secondary windings, which increases the leakage inductance and the layer capacitance of the secondary winding affecting the behavior of the converter. The turns-ratio of the transformer may be reduced to some extent by appropriately choosing the operating frequency and using the leakage inductance and the winding capacitance of the transformer wholly or partially as the resonant elements. Therefore, the transformer should be designed to satisfy the converter specifications and operate with high efficiency.

The converter parameters used in the simulation are corresponding to an X-ray generator design investigated in Eskandarzadeh (1996) with load specifications of 125 kV and 100 mA. The parameters of the high-voltage transformer designed in Eskandarzadeh (1996) have been obtained by developing an optimization program to minimize the volume of the transformer satisfying the load specifications. The program used in this optimization is GRG2 which solves nonlinear problems of the form of:

$$\text{minimize}: \quad f(x);$$
$$\text{subject to}: \quad \text{lb}f_i \le g_i(x) \le \text{ub}f_i \quad \text{and} \quad \text{lb}v_j \le x_j \le \text{ub}v_j$$

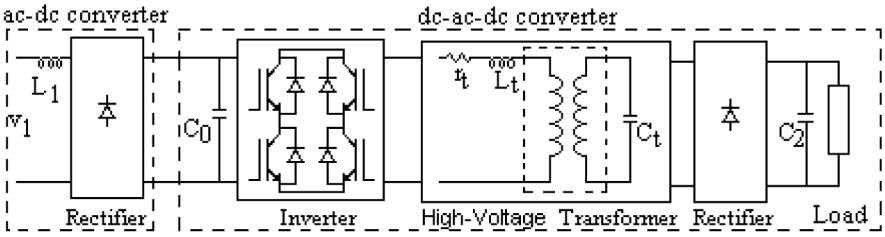

Figure 1.
Schematic diagram of the parallel resonant inverter-fed type high-voltage generator

where lb and ub represent lower and upper bounds of the corresponding function or variable, respectively. GRG2, solves the problems of the above form by generalized reduced gradient methods.

The transformer core is ferrite and the referred values of leakage inductance, stray capacitance, winding resistance and turns ratio obtained from the transformer design are 20.34 μH, 2.566 μF, 0.0015 Ω and 600, respectively. The results of investigation indicated that, for a ferrite core, the volume is minimized around 15 kHz and no further reduction in volume is achieved by further increasing the operating frequency.

3. Mathematical model of the system

The general mathematical model of the system is obtained by deriving and combining the mathematical models of the ac-dc and dc-ac-dc converters existing in the system. The model obtained is later used to study the steady-state and transient performance of the converter.

3.1 Input rectifier

The steady-state and transient behavior of the uncontrolled input rectifier can be described in three sub-modes as shown in Figure 2. The line inductance existing at the rectifier input (L_1) causes overlap to occur which affects the waveform and mean value of the rectifier output voltage. Since, the main idea of this paper is to study steady state operation of the dc-ac-dc converter not the ac-dc rectifier, so the overlap process is not focused in this paper.

The following equations can be written for the above operating modes.

Mode 1: D_1, D_4 are turned on and the capacitor C_0 is charging:

$$v_1 = L_1\left(\frac{\mathrm{d}i}{\mathrm{d}t}\right) + v_{C_0} \quad C_0\left(\frac{\mathrm{d}v_{C_0}}{\mathrm{d}t}\right) = i_1 - i_2 \quad v_{\mathrm{ab}} = v_{C_0} \quad i = i_1 \tag{1}$$

Mode 2: D_1, D_2, D_3, and D_4 are turned off and the capacitor C_0 is discharging. In this mode the rectifier is disconnected from the ac mains:

$$v_1 = v_{\mathrm{ab}} \quad C_0\left(\frac{\mathrm{d}v_{C_0}}{\mathrm{d}t}\right) = -i_2 \quad i = i_1 = 0 \tag{2}$$

Mode 3: D_2, D_3 are turned on and the capacitor C_0 is charging:

$$v_1 = L_1\left(\frac{\mathrm{d}i}{\mathrm{d}t}\right) - v_{C_0} \quad C_0\left(\frac{\mathrm{d}v_{C_0}}{\mathrm{d}t}\right) = i_1 - i_2 \quad v_{\mathrm{ab}} = -v_{C_0} \quad i = -i_1 \tag{3}$$

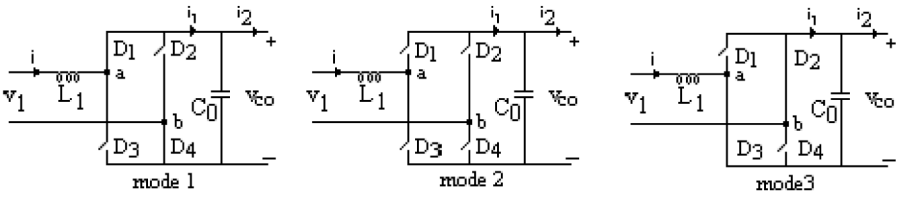

Figure 2.
Equivalent circuit of the input rectifier for different operating modes

3.2 DC-DC converter model

Figure 3 shows the dc-ac-dc converter including inverter, transformer and the output rectifier. The equivalent circuit of the transformer is shown by L_t, r_t and C_t corresponding to leakage inductance, winding resistance and winding capacitance of the transformer, respectively. The equivalent circuit of the converter depends on the on-off conditions of the inverter switches. The output dc voltage of the converter is controlled using PSPWM control method. In this method, the first leg switches (S_1, S_2) operate alternatively out of phase as reference switches and the second leg switches (S_3, S_4) also operate in the same manner, but with a phase shift angle (Φ) with respect to the first leg switches. By varying the phase shift angle from 180 to 0° the output dc voltage can be changed from zero to its peak value continuously. The symmetrical output voltage waveforms of the inverter are shown in Figure 4 for 0 and $\pi/3$ rad phase-shift angles.

The voltage at the primary side of the transformer, which has a square waveform is increased by the transformer and then rectified to feed the high-voltage load through the high-voltage cable whose capacitance may be utilized as smoothing capacitor in high-frequency operations.

The equivalent circuits of different operating modes of the dc-ac-dc converter corresponding to on-off operating state of the inverter switches and the output rectifier diodes are shown in Figure 5. The sequence of the converter operating modes corresponding to the intervals of 1, 2, 3, 4, 5, 6, 7 and 8 shown in Figure 6 is

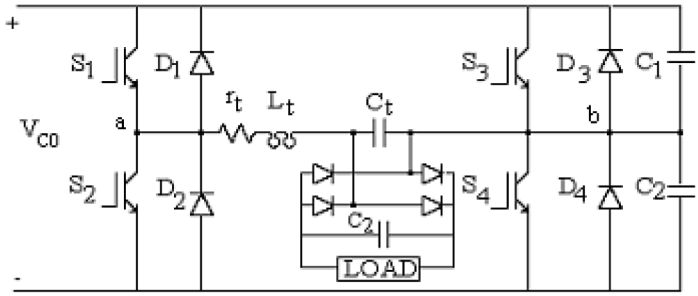

Figure 3.
Circuit diagram of the dc-ac-dc parallel resonant converter

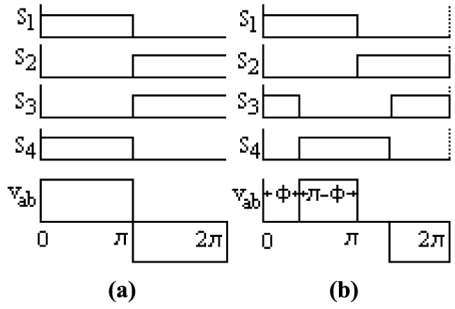

Notes: (a) phase-shift angle is zero; **(b)** phase-shift angle is π/3 rad

Figure 4.
Switching sequence in PSPWM control method

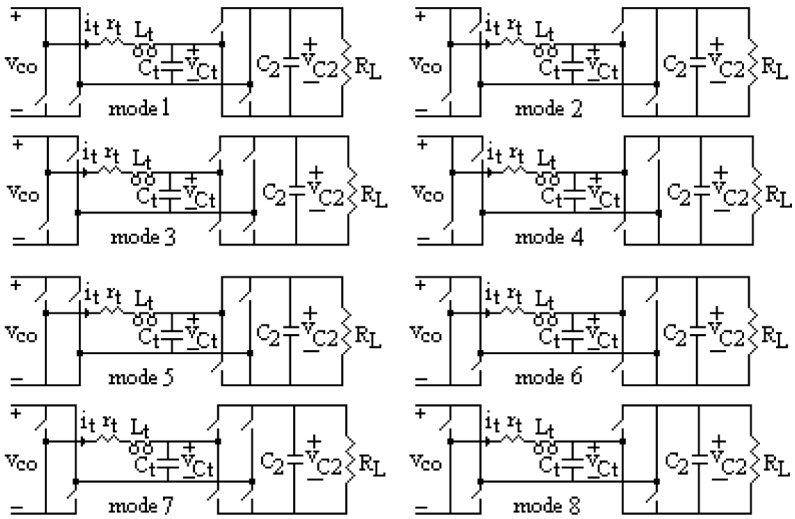

Figure 5.
Equivalent circuits of dc-ac-dc converter for different operating modes

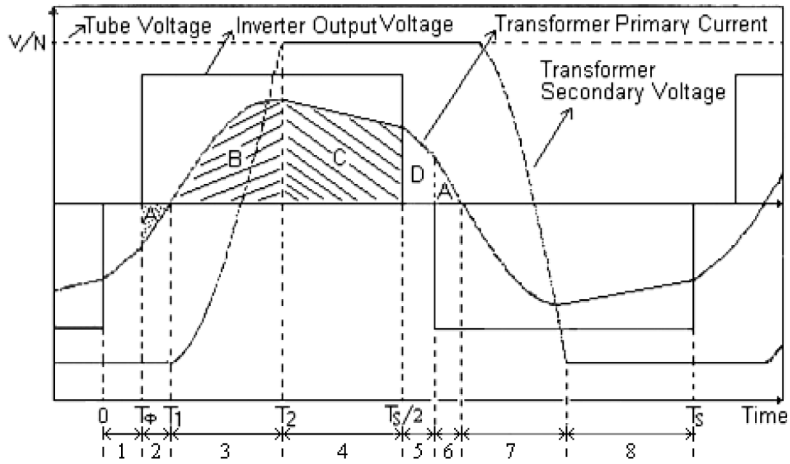

Figure 6.
Typical waveforms (tube voltage, output voltage of inverter, transformer current, transformer output voltage)

1, 2, 3, 4, 5, 6, 7 and 8, respectively, or, each operating mode and the corresponding interval have the same sequence number.

The following assumptions are made in deriving the analytical model of the dc-dc converter:

- switching devices, the inductor and the capacitors in the equivalent circuit of the converter are assumed to be ideal with no losses;
- wiring inductance and resistance are neglected;
- the X-ray tube is represented by a resistance corresponding to the ratio of the tube voltage to its current; and
- the load resistance and smoothing capacitance in the secondary side of transformer are referred to the primary side according to the transformer turns ratio.

The state equations corresponding to the circuit operation modes in Figure 5 can be written as:

Mode 1:

$$\frac{\mathrm{d}}{\mathrm{d}t}\begin{bmatrix} i_{\mathrm{t}} \\ v_{C_{\mathrm{t}}} \end{bmatrix} = \begin{bmatrix} -r_{\mathrm{t}}/L_{\mathrm{t}} & -1/L_{\mathrm{t}} \\ 1/C & -1/R_{\mathrm{L}}C \end{bmatrix}\begin{bmatrix} i_{\mathrm{t}} \\ v_{C_{\mathrm{t}}} \end{bmatrix} \quad v_{C_2} = -v_{C_{\mathrm{t}}}, \tag{4}$$

$$C = C_{\mathrm{t}} + C_2$$

Mode 2:

$$\frac{\mathrm{d}}{\mathrm{d}t}\begin{bmatrix} i_{\mathrm{t}} \\ v_{C_{\mathrm{t}}} \end{bmatrix} = \begin{bmatrix} -r_{\mathrm{t}}/L_{\mathrm{t}} & -1/L_{\mathrm{t}} \\ 1/C & -1/R_{\mathrm{L}}C \end{bmatrix}\begin{bmatrix} i_{\mathrm{t}} \\ v_{C_{\mathrm{t}}} \end{bmatrix} + \begin{bmatrix} v_{C_0}/L_{\mathrm{t}} \\ 0 \end{bmatrix} \quad v_{C_2} = -v_{C_{\mathrm{t}}}, \tag{5}$$

$$C = C_{\mathrm{t}} + C_2$$

Mode 3:

$$\frac{\mathrm{d}}{\mathrm{d}t}\begin{bmatrix} i_{\mathrm{t}} \\ v_{C_{\mathrm{t}}} \\ v_{C_2} \end{bmatrix} = \begin{bmatrix} -r_{\mathrm{t}}/L_{\mathrm{t}} & -1/L_{\mathrm{t}} & 0 \\ 1/C_{\mathrm{t}} & 0 & 0 \\ 0 & 0 & -1/R_{\mathrm{L}}C_2 \end{bmatrix}\begin{bmatrix} i_{\mathrm{t}} \\ v_{C_{\mathrm{t}}} \\ v_{C_2} \end{bmatrix} + \begin{bmatrix} v_{C_0}/L_{\mathrm{t}} \\ 0 \\ 0 \end{bmatrix} \tag{6}$$

Mode 4:

$$\frac{\mathrm{d}}{\mathrm{d}t}\begin{bmatrix} i_{\mathrm{t}} \\ v_{C_{\mathrm{t}}} \end{bmatrix} = \begin{bmatrix} -r_{\mathrm{t}}/L_{\mathrm{t}} & -1/L_{\mathrm{t}} \\ 1/C & -1/R_{\mathrm{L}}C \end{bmatrix}\begin{bmatrix} i_{\mathrm{t}} \\ v_{C_{\mathrm{t}}} \end{bmatrix} + \begin{bmatrix} v_{C_0}/L_{\mathrm{t}} \\ 0 \end{bmatrix} \quad v_{C_2} = v_{C_{\mathrm{t}}}, \tag{7}$$

$$C = C_{\mathrm{t}} + C_2$$

Mode 5:

$$\frac{\mathrm{d}}{\mathrm{d}t}\begin{bmatrix} i_{\mathrm{t}} \\ v_{C_{\mathrm{t}}} \end{bmatrix} = \begin{bmatrix} -r_{\mathrm{t}}/L_{\mathrm{t}} & -1/L_{\mathrm{t}} \\ 1/C & -1/R_{\mathrm{L}}C \end{bmatrix}\begin{bmatrix} i_{\mathrm{t}} \\ v_{C_{\mathrm{t}}} \end{bmatrix} \quad v_{C_2} = v_{C_{\mathrm{t}}}, \tag{8}$$

$$C = C_{\mathrm{t}} + C_2$$

Mode 6:

$$\frac{\mathrm{d}}{\mathrm{d}t}\begin{bmatrix} i_{\mathrm{t}} \\ v_{C_{\mathrm{t}}} \end{bmatrix} = \begin{bmatrix} -r_{\mathrm{t}}/L_{\mathrm{t}} & -1/L_{\mathrm{t}} \\ 1/C & -1/R_{\mathrm{L}}C \end{bmatrix}\begin{bmatrix} i_{\mathrm{t}} \\ v_{C_{\mathrm{t}}} \end{bmatrix} - \begin{bmatrix} v_{C_0}/L_{\mathrm{t}} \\ 0 \end{bmatrix} \quad v_{C_2} = v_{C_{\mathrm{t}}}, \tag{9}$$

$$C = C_{\mathrm{t}} + C_2$$

Mode 7:

$$\frac{\mathrm{d}}{\mathrm{d}t}\begin{bmatrix} i_{\mathrm{t}} \\ v_{C_{\mathrm{t}}} \\ v_{C_2} \end{bmatrix} = \begin{bmatrix} -r_{\mathrm{t}}/L_{\mathrm{t}} & -1/L_{\mathrm{t}} & 0 \\ 1/C_{\mathrm{t}} & 0 & 0 \\ 0 & 0 & -1/R_{\mathrm{L}}C_2 \end{bmatrix}\begin{bmatrix} i_{\mathrm{t}} \\ v_{C_{\mathrm{t}}} \\ v_{C_2} \end{bmatrix} - \begin{bmatrix} v_{C_0}/L_{\mathrm{t}} \\ 0 \\ 0 \end{bmatrix} \tag{10}$$

Mode 8:

$$\frac{\mathrm{d}}{\mathrm{d}t}\begin{bmatrix} i_{\mathrm{t}} \\ v_{C_{\mathrm{t}}} \end{bmatrix} = \begin{bmatrix} -r_{\mathrm{t}}/L_{\mathrm{t}} & -1/L_{\mathrm{t}} \\ 1/C & -1/R_{\mathrm{L}}C \end{bmatrix}\begin{bmatrix} i_{\mathrm{t}} \\ v_{C_{\mathrm{t}}} \end{bmatrix} - \begin{bmatrix} v_{C_0}/L_{\mathrm{t}} \\ 0 \end{bmatrix} \quad v_{C_2} = -v_{C_{\mathrm{t}}}, \quad C = C_{\mathrm{t}} + C_2 \tag{11}$$

4. Analytical model of the dc-ac-dc converter

The analytical model of the dc-ac-dc converter relating the dc-link and tube voltages to the phase-shift angle of the inverter is derived based on the steady-state operation conditions. The model can be used in estimating the output voltage of the converter. In deriving the analytical model of the converter, difficulties arise as a result of complicated and seemingly unsolvable algebraic equations of the converter, which can be removed by simplifying the equations.

The block diagram of the converter is shown in Figure 1. Elements L_{t}, C_{t}, C_0 and C_2 are assumed to be ideal. The filter element (C_2) is assumed to be large enough such that the high frequency ripple may be neglected. Typical waveforms of the converter are shown in Figure 6. Assuming the output voltage to be a waveform without ripple, $v_{C_{\mathrm{t}}}(t)$ can be expressed as:

$$v_{C_{\mathrm{t}}}(t) = \begin{cases} -V/N & 0 \le t \le T_\Phi \\ -V/N & T_\Phi \le t \le T_1 \\ \mathrm{v}_{C_0} - (\mathrm{v}_{C_0} + V/N)\cos\omega_o(t - T_1) & T_1 \le t \le T_2 \\ V/N & T_2 \le t \le T_{\mathrm{S}/2} \end{cases} \tag{12}$$

The transformer current can also be written as:

$$i_{\mathrm{L}}(t) = \begin{cases} i(0) + (V/N)t/L_{\mathrm{t}} & 0 \le t \le T_\Phi \\ i(\Phi) + (\mathrm{v}_{C_0} + V/N)(t - T_\Phi)/L_{\mathrm{t}} & T_\Phi \le t \le T_1 \\ C_{\mathrm{t}}\omega_{\mathrm{o}}(\mathrm{v}_{C_0} + V/N)\sin\omega_{\mathrm{o}}(t - T_1) & T_1 \le t \le T_2 \\ i(T_2) + (\mathrm{v}_{C_0} - V/N)(t - T_2)/L_{\mathrm{t}} & T_2 \le t \le T_{\mathrm{S}/2} \end{cases} \tag{13}$$

where V is the output voltage of converter, N is the turns ratio of the transformer, v_{C_0} is the dc-link voltage, L_{t} is the transformer leakage inductance, C_{t} is the transformer layer capacitance, f_{S} is the switching frequency, $T_{\mathrm{S}} = 1/f_{\mathrm{S}}$, $\omega_{\mathrm{o}} = 1/\sqrt{L_{\mathrm{t}}C_{\mathrm{t}}}$, R_{L} is load value referred to the primary

The beginning and end of the subintervals are shown by (0, T_Φ), (T_Φ, T_1), (T_1, T_2) and (T_2, $T_{\mathrm{S}}/2$), respectively. Using the boundary conditions, i.e. equating the initial and final values of the variables corresponding to different subintervals, the following relations are obtained:

$$i(0) + \frac{(V/N)T_\Phi}{L_t} = i(\Phi) \tag{14}$$

$$i(\Phi) + \frac{(v_{C_0} + V/N)(T_1 - T_\Phi)}{L_t} = 0 \tag{15}$$

$$C_t\omega_o(v_{C_0} + V/N)\sin\omega_o(T_2 - T_1) = i(T_2) \tag{16}$$

$$i(T_2) + \frac{(v_{C_0} - V/N)(T_S/2 - T_2)}{L_t} = i(T_S/2) = -i(0) \tag{17}$$

$$v_{C_0} - (v_{C_0} + V/N)\cos\omega_o(T_2 - T_1) = V/N \tag{18}$$

$$\cos\omega_o(T_2 - T_1) = \frac{(v_{C_0} - V/N)}{(v_{C_0} + V/N)} \tag{19}$$

Defining $\alpha = \omega_o(T_2 - T_1)$, the parameters $i(0)$, $i(\Phi)$, T_2, $i(T_2)$ and T_1 can be obtained as a function of T_Φ as:

$$T_1 = \left(\frac{L_t}{2v_{C_0}}\right)\left[\frac{C_t\omega_o(v_{C_0}+V/N)\sin\alpha + (v_{C_0}-V/N)(T_S/2-\alpha/\omega_o)}{L_t} + \left(\frac{v_{C_0}}{L_t}\right)T_\Phi\right] \tag{20}$$

$$\begin{aligned} i(\Phi) = \Big(&-(v_{C_0}+V/N)\{(L_t/2v_{C_0})[C_t\omega_o(v_{C_0}+V/N)\sin\alpha \\ &+(v_{C_0}-V/N)(T_S/2-\alpha/\omega_o)/L_t + (v_{C_0}/L_t)T_\Phi] - T_\Phi\}\Big) \Big/ \Big(L_t\Big) \end{aligned} \tag{21}$$

$$\begin{aligned} i(0) = \Big(&-(V/L_t)T_\Phi - (v_{C_0}+V/N)\{(L_t/2v_{C_0})[C_t\omega_o(v_{C_0}+V/N)\sin\alpha \\ &+(v_{C_0}-V/N)(T_S/2-\alpha/\omega_o)/L_t + (v_{C_0}/L_t)T_\Phi] - T_\Phi\}\Big) \Big/ \Big(L_t\Big) \end{aligned} \tag{22}$$

$$\begin{aligned} T_2 = \left(\frac{\alpha}{\omega_o}\right) + \left(\frac{L_t}{2v_{C_0}}\right)\Bigg[&C_t\omega_o\left(v_{C_0}+\frac{V}{N}\right)\sin\alpha \\ &+\left(v_{C_0}-\frac{V}{N}\right)\frac{(T_S/2-\alpha/\omega_o)}{L_t} + \left(\frac{v_{C_0}}{L_t}\right)T_\Phi\Bigg] \end{aligned} \tag{23}$$

$$i(T_2) = C_t\omega_o\left(v_{C_0}+\frac{V}{N}\right)\sin\alpha \tag{24}$$

Using Figure 6 and assuming the dc-ac-dc converter to be lossless, the following relations are obtained:

$$\text{Input Average Active Power} = \text{Output Power} \tag{25}$$

$$\frac{2v_{C_0}(-A+B+C)}{T_S}=\left[\frac{(V/N)^2}{R_L}\right] \tag{26}$$

where A, B and C are areas as shown in Figure 6.

V/N is the converter output voltage referred to the primary side of the transformer ($V_{C_2} = V/N$). The voltage gain of the dc-ac-dc converter referred to the primary side of the transformer is equal to V_{C_2}/v_{C_0} (or V/Nv_{C_0}), where V, N, V_{C_2} and v_{C_0} are the converter output voltage, transformer turns ratio, converter output voltage referred to the primary and dc-link voltage, respectively. Defining $M = V/Nv_{C_0}$, $1 + M = M_1$ and $1 - M = M_2$ and using Figure 6, the areas A, B and C are determined as:

$$A = \left(\frac{v_{C_0}M_1}{8L_t\omega_o^2}\right)[M1\sin\alpha + M_2(\gamma-\alpha) - \omega_o T_\Phi]^2 \tag{27}$$

$$B = C_t v_{C_0} M_1(1 - \cos\alpha) \tag{28}$$

$$\begin{aligned} C = &\left[C_t\omega_o v_{C_0}M_1\sin\alpha + \left(\frac{v_{C_0}M_1}{2L_t\omega_o}\right)\right]\left[M_1\sin\alpha + M_2(\gamma-\alpha) - \left(\frac{M_2}{M_1}\right)\omega_o T_\Phi\right] \\ &*\left\{\frac{1}{f_S} - (1/2\omega_o)[M_1\sin\alpha + M_2(\gamma-\alpha) + 2\alpha + \omega_o T_\Phi]\right\} \end{aligned} \tag{29}$$

where $\gamma = \pi/F$, $F = f_S/f_o$, f_o = resonant frequency

Substituting A, B and C into equation (26) and simplifying it, a second order function is obtained as follows:

$$K_1 T_\Phi^2 + K_2 T_\Phi + K_3 = 0 \tag{30}$$

The coefficients K_1, K_2 and K_3 which are functions of v_{C_0} and V can be obtained as:

$$K_1 = -\left(\frac{v_{C_0}M}{4L_t}\right)$$

$$K_2 = 0$$

$$K_3 = \left(\frac{v_{C_0}M}{4L_t\omega_o^2}\right)\left[-4M + (1-M^2)(\gamma-\alpha)^2 + 4\sqrt{M}(1+M)(\gamma-\alpha) - \frac{4L_t\omega_o M\gamma}{R_L}\right]$$

By solving equation (30), T_Φ is obtained as:

$$T_\Phi^2 = \left(\frac{1}{\omega_o^2}\right)\left[-4M + (1-M^2)(\gamma-\alpha)^2 + 4\sqrt{M}(1+M)(\gamma-\alpha) - \frac{4L_t\omega_o M\gamma}{R_L}\right] \tag{31}$$

The above equation can be rewritten as:

$$T_\Phi = \left(\frac{1}{\omega_o}\right)\sqrt{A' - B'M} \tag{32}$$

where A' and B' are:

$$A' = (1 - M^2)(\gamma - \alpha)^2 + 4\sqrt{M}(1 + M)(\gamma - \alpha) \tag{33}$$

$$B' = 4\left(1 + \frac{L_t \omega_o \gamma}{R_L}\right) \tag{34}$$

The parameter A' depends on M and there is a complicated relation between parameter A' and M (equation (33)) which can be simplified. For this purpose, a line is fitted for parameter A' (equation (33)) in the range between 30 and 100 percent of the rated value of the tube voltage. The parameters of the fitted line (equation (35)) are obtained using least-square line method as:

$$A'(\text{simplified}) = 2.383M + 21.845 \tag{35}$$

Substituting A' and B' into equation (32) gives:

$$T_\Phi = \left(\frac{1}{\omega_o}\right)\sqrt{C' - D'M} \tag{36}$$

where:

$$C' = 21.845$$

$$D' = \left(\frac{4L_t \omega_o \gamma}{R_L} + 1.617\right)$$

From equation (36), M is derived as:

$$M = \left(\frac{C' - T_\Phi^2 \omega_o^2}{D'}\right) \tag{37}$$

The relationship between T_Φ (time corresponding to phase-shift angle) and phase-shift angle is given by equation (38).

$$T_\Phi = \left(\frac{\text{phase} - \text{shift angle}}{f_S 2\pi}\right) \tag{38}$$

Combining equations (37) and (38) gives:

$$M = \left[\frac{[C' - (\text{phase} - \text{shift angle})^2 / F^2]}{D'}\right] \tag{39}$$

$$\text{Phase} - \text{shift angle(rad)} = F\sqrt{C' - D'M} \tag{40}$$

Using equations (39) and (40) it is possible to determine M (the primary side voltage gain of the dc-ac-dc converter) and the phase-shift angle with respect to each other for any value of dc-link voltage.

5. Simulation software and results

To verify the analytical model of the dc-ac-dc converter obtained in the previous section, a simulation software program was developed in Pascal Language and used to

solve the state equations (4-11) using the fourth order Runge-Kutta numerical method. The transformer equivalent circuit parameters used in this simulation are given in Section 2. The values of the referred load resistance (R_L), referred output filter capacitance (C_2), dc-link voltage (v_{C_0}) and the switching frequency (f_S) used in the simulation are 3·472 Ω, 60 μF, 160 V and 15 kHz, respectively. The inverter and the rectifier used in the simulation are single phase bridge connected converters.

The software program used in this simulation is consisting of three subroutines that are called from the main program (Main). The first subroutine is used to read the input data such as: the converter components values, operating frequency, load value .... The equations corresponding to different operating modes are solved in the second subroutine. In the third subroutine, the data obtained from solving the equations are recorded in a data file and evaluated to be monitored on the computer screen.

The intervals corresponding to different operating modes are determined considering the initial and final conditions of the corresponding operating modes. During interval 1 switch S_1 and S_3 are in conduction state and the current of the transformer primary is negative. The differential equations describing the system during this interval are given in equation (4). This interval ends when switch S_3 is turned off and switch S_4 is turned on. Interval 2 begins after interval 1 and ends when the transformer primary current becomes positive or the rectifier current decreases to zero. During this interval switches S_1 and S_4 are in conduction state and the equivalent circuit of converter is described by equation (5). Interval 3 begins after Interval 2 and ends when C_t and C_2 voltages become equal in value. During this interval, the inverter and the output rectifier circuit are independent (all the rectifier diodes are in off state) and the equivalent circuit of the converter is described by equation (6). Interval 4 follows Interval 3 in a sequence. The equivalent circuit of the converter in this interval is described by equation (7). This interval ends when switch S_4 is turned off and S3 is turned on. The equivalent circuits of the converter during the second half-cycle of the operation are shown in Figure 5, modes 5, 6, 7 and 8 corresponding to intervals 5, 6, 7 and 8 shown in Figure 6, respectively.

The simulation results are compared with the results obtained using the analytical model. Figure 7 shows the variation of the dc-ac-dc converter voltage gain referred to transformer primary ($M = V_{C_2}/v_{C_0}$) with respect to the phase-shift angle of the converter for two different cases using:

- simulation software program; and
- analytical model.

It is shown that the error decreases with increasing M. The error is 4 percent when the output voltage is 30 percent of the rated output voltage and is zero when the output voltage is equal to the rated output voltage (output voltage for zero phase-shift angle). The average error for the output voltage higher than 30 percent of the output voltage rated value (for the operations with phase shift angle in the range of 0 to 140°) is less than 0.35 percent.

The variation of M was studied for different cases of operation using simulation software program. Figure 8 shows the referred output voltage and dc-link voltage of the overall system combined of ac-dc and dc-ac-dc converters (equations (1-11)) corresponding to one of these cases. In this case of operation, the system is supplied by the ac mains, the dc-link capacitor has an arbitrarily chosen initial voltage of 140 V and

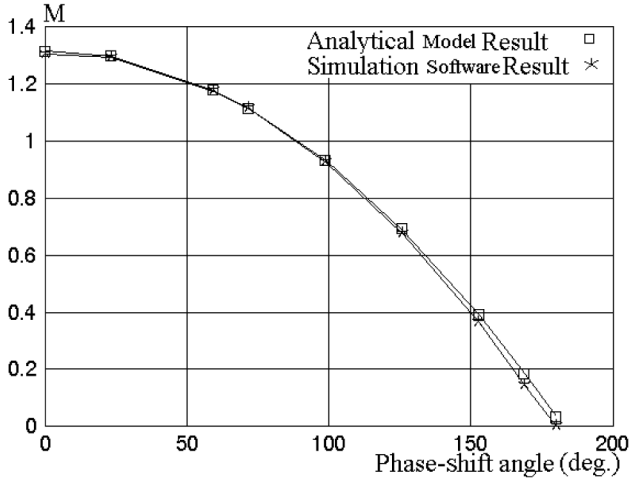

Figure 7.
Relationship between M and phase-shift angle predicted from equation (39) and simulation software program

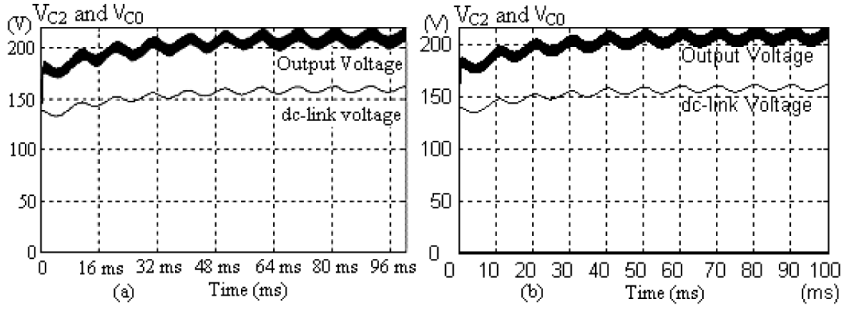

Figure 8.
Referred tube voltage, dc-link voltage (Phase-shift angle $= 0°$ and $v_{C_0}(0) = 140$ V)

Notes: (a) obtained from authors' software program; **(b)** obtained from MATLAB/SIMULINK

the phase-shift angle is constant and is equal to zero. It is shown that the output voltage traces the dc-link voltage in such a way that the ratio of the tube voltage to the dc-link voltage is always constant. Figure 8(a) and (b) are the simulation results obtained from authors' software program and the MATLAB/SIMULINK, respectively.

6. Experimental results

The set up of the experiments used in the laboratory is shown in Figure 9. The inverter and the rectifier are single-phase bridge consisting of four IGBTs and four fast recovery diodes, respectively. L_t, C_t and r_t are the leakage inductance, secondary layer capacitance and transformer winding resistance referred to the primary, respectively, and their values are given in Section 2 of this paper. The values of the referred load resistance (R_L), referred output filter capacitance (C_2) and the switching frequency (f_S) are given in the Section 5. The phase-shift angle of the signals is adjusted by the microcontroller and sent to the inverter switches through an interface circuit.

The experiments were carried out for different values of dc-link voltage to investigate the relationship between M and the phase-shift angle of the inverter.

The results of these experiments show that the variation of M does not depend on the dc-link voltage level but depends only on the phase-shift angle of the inverter. In one of these experiments the dc-link voltage was adjusted to 25 V and the output voltage was measured for the different values of the phase-shift angle while the dc-link voltage was kept constant during the experiment. The ratio of the output voltage to the dc-link voltage (M) was determined for different phase shift angles. The inverter switches used in this experiment are intelligent power module (IPM) dual type manufactured by Mitsubishi Electric (PM200DSA060).

The dead time required for the IPM used in this experiment is 3.5 μs. Considering an additional dead time of 2 μs for the safety operation, the experiment was carried out for dead time of 5.5 μs which corresponds to a phase-shift angle of 29.5° for an operating frequency of 15 kHz. In experiment, the non-idealities of the converter such as voltage drop on the inverter switches and the rectifier diodes were taken into account. Figure 10(a) shows the variation of M versus the phase-shift angle of the converter. In this figure, the results obtained from the experiment are compared with those corresponding to the analytical model. The minimum value of the phase-shift angle of the signals applied to the switches of the inverter is 30° due to 5.5 μs dead time of the inverter switches. The discrepancy between the experimental results and the results obtained from the analytical model increases for the phase shift angles greater than 140°. The errors corresponding to the phase-shift angles of 140 and 30° are 4.2 and 0.65 percent, respectively. The average error corresponding to the output voltage in the range of higher than 30 percent of the output rated value (or for the phase-shift angles in the range of 30 to 140°) is less than 1 percent.

To decrease the dead time of the inverter legs switches, another experiment was performed in which the dc-link voltage was adjusted to 100 V and the inverter switches were replaced with IGBT of the IRG4PSC71UD manufactured by International Rectifier. The dead time was adjusted to 2 μs which is corresponding to a phase-shift angle of 10.8° for the operating frequency of 15 kHz. During this experiment, the dc-link voltage was kept constant at 100 V and the output voltage of the converter was measured for different values of phase shift angle in the range of 10.8 to 170°. The voltage gain of the converter (M) was derived for different values of phase shift angles considering the dc-link voltage, converter output voltages, voltage drop on the inverter switches and voltage drop on the output rectifier diodes (IXYS DSEI 60, 600 V). The results of this experiment (Figure 10(b)) are similar to the results of the first one (Figure 10(a)). The discrepancy between the analytical and practical results increases with increasing the phase shift angle beyond 140°. The average error for the phase shift angle less than 140° is about 1.2 percent. The specifications of the inverter switches, output rectifier diodes used in experiments are given in the Appendix of this paper.

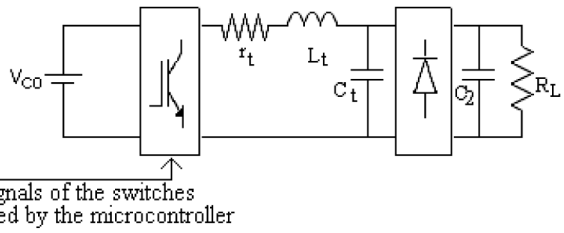

Figure 9.
The experimental set up

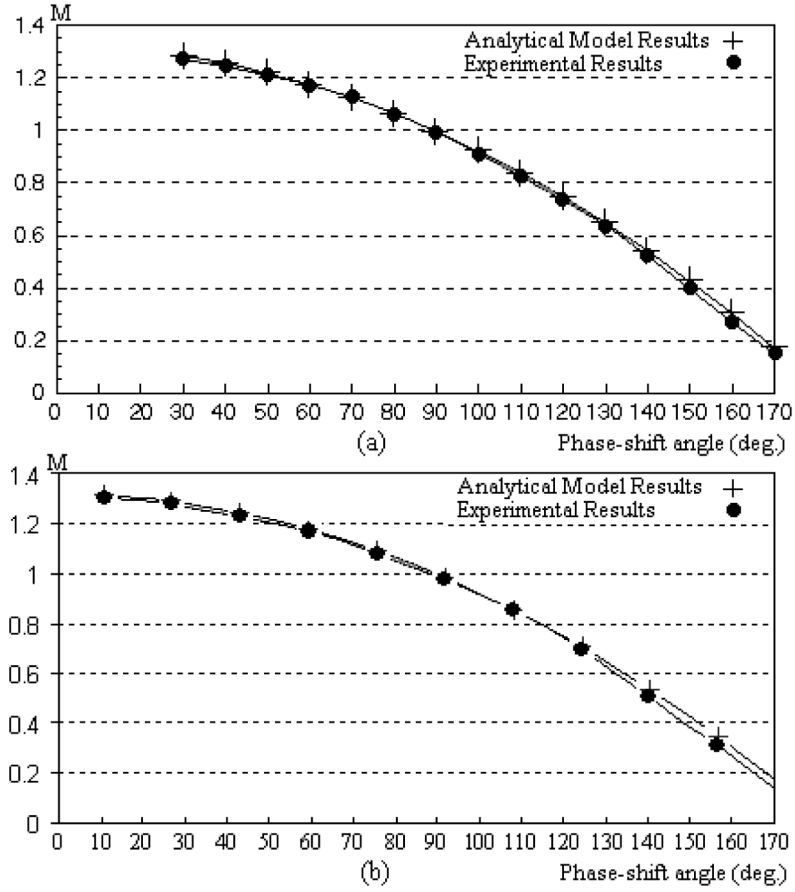

Figure 10.
Variation of M versus the phase-shift angle of the converter for the cases: (a) dc-link voltage of 25 V and inverter switches of the PM200DSA060 (b) dc-link voltage of 100 V and inverter switches of the IRG4PSC71UD

7. Conclusions

The dynamic and steady-state analysis of a dc-ac-dc parallel resonant converter have been presented in this paper. The results obtained from the software simulation and the hardware implemented in the laboratory indicate that the analytical model of the converter obtained using the steady-state solutions of the system performs well in predicting the output voltage in terms of phase-shift angle. The error remains within 1.2 percent for the load voltage values higher than 30 percent of the rated output voltage. The use of the proposed method is not restricted to high voltage applications, but also can be used in output voltage estimation of dc-ac-dc parallel resonant converters.

The decrease in the accuracy of the results obtained using the analytical model of the dc-ac-dc converter is due to some assumptions made in deriving the analytical model such as neglecting the ripple on the output voltage and simplifying assumptions which are used in curve fitting. The proposed model can be successfully used in dc-ac-dc applications with the phase angle in the range of 0 to 140° (or, in the applications where the needed output voltage is greater than 30 percent of the output

voltage rated value). For the applications with output voltage less than 30 percent of the output voltage rated value, the model can be used at its desired region (phase-shift angle between 0 and 140°) if dc-link voltage can be reduced below its rated value and this will be possible using a controlled rectifier (ac-dc converter) at the input of the dc-ac-dc converter.

Though the voltage drops on the inverter switches and the output rectifier diodes have been considered in the evaluation of the experimental results, the non-ideal properties of the elements used in the experiments still have some role in the discrepancy between the experimental results and those corresponding to the analytical model.

References

Bhat, A.K.S. and Swamny, M.M. (1990), "Analysis and design of a parallel resonant converter including the effect of a high-frequency transformer", *IEEE Trans. Industrial Electronics*, Vol. 37 No. 4.

Eskandarzadeh, I. (1996), "Design and control of a phase-shift PWM resonant converter for an X-ray generator", PhD thesis, Department of Electrical & Electronics Engineering, University of Middle East Technical, Ankara, December.

Sooksatra, S. and Lee, C.Q. (1989), "Non-resonant coupled parallel resonant converter", paper presented at IEEE 32nd Symp. Circuits Syst., pp. 781-4.

Steigerwald, R.L. (1984), "High-frequency resonant transistor DC-DC converters", *IEEE Trans. Industrial Electronics*, Vol. IE-31 No. 2, pp. 181-91.

Steigerwald, R.L. (1985), "Analysis of a resonant transistor DC-DC converter with capacitive output filter", *IEEE Trans. On Industrial Electronics*, Vol. IE-32 No. 4, pp. 439-44.

Steigerwald, R.L. (1988), "A comparison of half-bridge resonant converter topologies", *IEEE Trans. Power Electronics*, Vol. 3 No. 2, pp. 174-82.

Sun, J.M., Takano, H. and Nakaoka, M. (1996), "Transformer parasitic high-frequency inverter-fed DC-DC converter for medical-use X-ray power generator and its digital control", *Proceeding of IEEE International Conference on Industrial Technology (ICIT), China, December*, pp. 400-5.

Takano, H., Takahashi, J., Hatakeyama, T. and Nakaoka, M. (1995), "Feasible characteristic evaluations of resonant tank PWM-inverter-linked DC-DC high-voltage converters for medical-use high-voltage application", *Proceedings of IEEE-APEC*, Vol. 2, p. 913.

Appendix

The parameters of the converter used in the simulation and experiments are as:

L_t (leakage inductance of the transformer) $= 20.34\,\mu$H.

C_t (capacitance of the transformer windings) $= 2.566\,\mu$F.

N (turns ratio of the transformer) $= 600$.

r_t (resistance of the transformer windings) $= 0.0015\,\Omega$.

R_L (load referred to the primary side of the transformer) $= 3.472\,\Omega$.

C_2 (output filter capacitor) $= 60\,\mu$F.

f_o (operating frequency) $= 15$ kHz.

The specifications of the inverter switches and the output rectifier diodes are as:

The inverter switches of the first experiment are IPM dual type manufactured by Mitsubishi Electric (PM200DSA060).

The output rectifier diodes are: fast recover diode, IXYS DSEI 60 A, 600 V, $t_{rr} = 35$ ns.

Voltage drop on the diode using the *i-v* characteristics of the diode is 1.25 V.

The inverter switches of the second experiment are International Rectifier IGBT IRG4PS71UD manufactured by International Rectifier with the following specifications:

$V_{CES} = 600$ V.

I (continuous current at 25°C = 80 A, at 100°C = 60 A).

$V_{CE(on)} = 1.67$ V.

The specifications of the transformer designed in Eskandarzadeh (1996) are as:

Turns number of primary = 11.

Turns number of secondary = 6,542.

Leakage inductance = 20.34 μH.

The secondary layers capacitance = 2.566 μF.

Current density = 180 A/cm^2.

Efficiency = 0.988.

Secondary winding layers number = 45.

Primary winding layers number = 1.

Number of conductors in one layer of the secondary winding = 145.

Number of conductors in one layer of the primary winding = 11.

Diameter of the primary conductors = 0.808 cm.

Diameter of the secondary conductor = 0.0324 cm.

Transformer volume = 7,480 cm^3

Core of the transformer is ferrite.

Transformer dimensions (Units: cm)

Corresponding author

İres İskender can be contacted at: iresis@gazi.edu.tr